Deterministic Measurement Procedures for Diagnosis of Massive Uniform Linear Antenna Arrays

M. Mokhtar*, R. Hamila*, W. U. Bajwa† and N. Al-Dhahir‡
*Qatar University, Qatar, {m.mokhtar, hamila}@qu.edu.qa
†Rutgers, The State University of New Jersey, USA, waheed.bajwa@rutgers.edu
‡University of Texas at Dallas, USA, aldhahir@utdallas.edu

***Abstract*—The number and relative geometry of collected measurements significantly affect the reliability of massive antenna array diagnosis. In this paper, we investigate and compare two deterministic algorithms for taking measurements based on a compressive-sensing-based approach for rapid and reliable detection of faulty elements in massive multi-input multi-output antenna arrays. We exploit the fact that the measurement matrix for a uniform linear antenna array reduces to a partial discrete Fourier transform matrix with rows corresponding to the measurements' locations. With the aid of the investigated algorithms, the measurements can be wisely taken to reduce the measurement matrix's worst-case coherence, which affects the detection probability of the defective antenna elements. In particular, one of the algorithms aims at constructing a measurement matrix with fewer distinct inner product values to reduce the worst-case coherence. The second algorithm is based on bounding the inner product between any pair of measurement matrix columns. Our study shows that uniform measurements can adversely affect the detection probability of the defective antenna elements, while using either one of the investigated deterministic algorithms leads to remarkable performance improvement.**

I. Introduction

Very large multiple-input multiple-output (MIMO) systems, widely known as massive MIMO, have gained an increasing attention in academic and industrial circles as one of the key enabling technologies for the 5G cellular systems [1]. They offer substantial performance gains over traditional MIMO systems such as increasing the system throughput by allowing multiple user equipment to be scheduled simultaneously over the same time-frequency resources and enabling transmission of multiple independent data streams to fully exploit all available spatial degrees of freedom. Moreover, massive MIMO mitigates inter-user interference by creating narrow beams directed to the receiver of interest and extends the cell radius by focusing the transmitted power in such spatial directions. Furthermore, it permits significant power reduction by coherently combining the transmitted or received signals.

To realize these performance gains, several schemes have been proposed to design the precoder and decoder matrices. Those schemes assume the massive MIMO antenna array elements to be fault free. In practice, with large antenna arrays consisting of low-cost antenna elements, the presence of faulty antenna elements with excitation coefficients different from the designed ones may occur with high probability. Such faults result in significant deviation from the designed array radiation pattern and can lead to severe performance degradation.

Several array diagnosis schemes have been proposed in the literature to detect faulty antenna elements and compensate for their detrimental effects on the performance. Backward method array diagnosis based on the inverse fast Fourier transform (FFT) was proposed in [2]. To obtain reliable diagnosis using this scheme, a very large number of measuremts must be collected in the measurement plane. In [3], another technique based on the "matrix method" was proposed to reconstruct the excitation coefficients. The main drawback of this technique is that the number of measurements has to be bigger than the number of antenna elements in the array, which requires tremendous time to collect measurements for large antenna arrays. A spectral estimation technique based on the Multiple Signal Classification (MUSIC) method was presented in [4]; it is based on singular value decomposition (SVD), which is not practical for large antenna arrays.

To reduce the number of measurements and enhance the reliability of detecting defective antenna elements, array diagnosis schemes based on compressive sensing (CS) have been recently proposed. They exploit the fact that only few antenna elements tend to be defective compared with the total number of elements and, hence, the difference between the excitation coefficients of the array under test and the reference array is a sparse vector that can be recovered using conventional CS recovery algorithms. In [5], identifying the faulty antenna elements from near-field measurements based on CS techniques was achieved by minimizing the l_1 norm. A Bayesian CS recovery approach for linear antenna arrays was proposed in [6] and generalized for planar arrays in [7].

To the best of the authors' knowledge, this paper is the first to address the problem of measurement collection procedures for array diagnosis based on CS techniques for massive unifrom linear antenna arrays (ULAs). In related work [5]–[7], and the references therein, the measurements were assumed to be uniformely collected and nonuniform sampling has not been investigated before. The main contributions of this paper are as follows. First, for a prime number of antenna elements, we present an algorithm to select the measurement positions based on the approach outlined in [8] when the number of measurements is any divisor of the number of antenna elements-1. Second, when this condition is not satisfied, we describe another algorithm based on the approach in [9]. Third, through extensive numerical simulations, we demonstrate the performance gains of the presented algorithms over the conventional uniformly-sampled measurements that result in poor performance in terms of detection probability.

The rest of the paper is organized as follows. In Section II, we present a brief background on CS, develop our system model and state our main assumptions. The proposed measurements procedures are described in Section III, followed by numerical simulations in Section IV. Finally, the paper is concluded in Section V.

This publication was made possible by NPRP grant # NPRP 6-070-2-024 from the Qatar National Research Fund (a member of Qatar Foundation). The statements made herein are solely the responsibility of the authors

II. CS Recovery Background and System Model

A. CS Recovery Background

Based on CS techniques, a sparse U-dimensional signal vector $\mathbf{x}$ with κ nonzero entries such that $\kappa \ll U$ can be efficiently and reliably estimated from N noisy linear measurements where $N < U$. The stacked N measurements can be denoted by vector $\mathbf{y} \in \mathbb{C}^N$ and written as follows

$$\mathbf{y} = \mathbf{\Phi}\mathbf{x} + \mathbf{w}, \tag{1}$$

where $\mathbf{\Phi}$ is an $N \times U$ measurement matrix and $\mathbf{w}$ is $N \times 1$ noise vector. An estimate of the sparse vector $\mathbf{x}$ can be obtained by solving the following optimization problem

$$\hat{\mathbf{x}} \triangleq \underset{\mathbf{x}\in\mathbb{C}^U}{\arg\min} \ \|\mathbf{x}\|_0 \quad \text{subject to} \quad \|\mathbf{y} - \mathbf{\Phi}\mathbf{x}\|_2^2 \leq \epsilon \tag{2}$$

where $\|\mathbf{x}\|_0$ is the l_0 norm of the vector $\mathbf{x}$, which counts its nonzero entries, and ϵ is chosen large enough to bound the measurement noise with high probability.

Recovering the locations of the κ nonzero entries of $\mathbf{x}$ depends on the characteristics of the measurement matrix $\mathbf{\Phi}$. Several metrics have been developed to assess the quality of the measurement matrix to enable stable and reliable recovery of the support of $\mathbf{x}$, such as the restricted isometry property (RIP), average coherence, and worst-case coherence [10]. In this paper, we focus on the worst-case coherence as a coherence measure between the measurement matrix's columns, which is defined as follows

$$\mu = \max_{i,j:i\neq j} \frac{\left|\boldsymbol{\phi}_i^H \boldsymbol{\phi}_j\right|}{\|\boldsymbol{\phi}_i\|_2 \|\boldsymbol{\phi}_j\|_2}, \tag{3}$$

where the operators $(.)^H$, $|.|$ and $\|.\|_2$ denote the matrix complex-conjugate transpose, absolute value of a complex number and the l_2 vector norm, respectively. Moreover, $\boldsymbol{\phi}_i \in \mathbb{C}^N$ denotes the i^{th} column of the matrix $\mathbf{\Phi}$.

The well-known lower-bound on the worst-case coherence, called the Welch bound, is given by [11]

$$\mu \geq \sqrt{\frac{U-N}{(U-1)N}} \tag{4}$$

with equality if and only if $\left|\boldsymbol{\phi}_i^H \boldsymbol{\phi}_j\right| = \sqrt{\frac{U-N}{(U-1)N}} \ \forall \ i \neq \ j$. The closer the worst-case coherence of the constructed measurement matrix is to the Welch bound, the more reliable the recovering of the nonzero entries will be.

B. System Model

Let us consider a linear antenna array consisting of U antenna elements located on the x-axis. The position of the u^{th} antenna element is denoted by x_u. Moreover, the excitation coefficient of the u^{th} antenna element is denoted by c_u. Suppose there are κ faulty antenna elements with unknown locations, where $\kappa \ll U$; i.e., their excitation coefficients are not equal to the true ones.

To detect the faulty antenna elements, N far-field measurements are collected, where the $(n+1)^{\text{th}}$ measurement is $v_{n+1} = \sum_{u=1}^{U} c_u \frac{\mathrm{e}^{-jkr_{un}} \overrightarrow{f_u}(\overrightarrow{r}_{un}, \theta_n, \phi_n)}{4\pi r_{un}} + w_n$, where $n \in \{0, \ 1, \cdots, \ N-1\}$, $j = \sqrt{-1}$ and $k = \frac{2\pi}{\lambda}$ is the wave number with λ being the free-space wavelength. The vector $\overrightarrow{f_u}(\overrightarrow{r}_{un}, \theta_n, \phi_n)$ is the electric field radiation pattern of the u^{th} antenna element at the $(n+1)^{\text{th}}$ measurement point and $r_{un} = |\overrightarrow{r}_{un}| = |\overrightarrow{r}_n - \overrightarrow{r}_u|$, where $\overrightarrow{r}_u$ and $\overrightarrow{r}_n$ are the position vectors of the u^{th} antenna element and the $(n+1)^{\text{th}}$ measurement point, respectively. The azimuth and elevation angles of the probe at the $(n+1)^{\text{th}}$ position are denoted by ϕ_n and $90^\circ - \theta_n$, respectively. Moreover, w_n denotes the measurement noise of the $(n+1)^{\text{th}}$ measurement. The noise samples over all the measurements are assumed to be independent, identically distributed (i.i.d) zero-mean additive white Gaussian noise (AWGN) samples with variance σ_w^2.

The N measurements are collected in a measurement vector $\mathbf{v} \in \mathbb{C}^N$, termed as ***the measurement vector***, given by

$$\mathbf{v} = \mathbf{A}\mathbf{c} + \mathbf{w}, \tag{5}$$

where the $(n+1, \ u)^{\text{th}}$ entry of the $N \times U$ ***measurement matrix*** $\mathbf{A}$ is given by $\frac{\mathrm{e}^{-jkr_{un}} \overrightarrow{f_u}(\overrightarrow{r}_{un}, \theta_n, \phi_n)}{4\pi r_{un}}$, the $U \times 1$ vector $\mathbf{c}$ consists of the excitation coefficients of the antenna array elements, i.e., $\mathbf{c} = [c_1, \ \cdots, \ c_U]^T$ and vector $\mathbf{w} = [w_0, \ \cdots, \ w_{N-1}]^T$. Denoting the error-free antenna elements' excitation coefficients by $\mathbf{c}_{\text{T}} \in \mathbb{C}^M$ and subtracting the ideal radiation pattern at the N measurement positions given by $\mathbf{v}_{\text{T}} = \mathbf{A}\mathbf{c}_{\text{T}}$ from (5), we get

$$\underbrace{\mathbf{v} - \mathbf{v}_{\text{T}}}_{\tilde{\mathbf{v}}} = \mathbf{A}\underbrace{(\mathbf{c} - \mathbf{c}_{\text{T}})}_{\tilde{\mathbf{c}}} + \mathbf{w}, \tag{6}$$

where the indices of the κ nonzero entries of $\tilde{\mathbf{c}}$ indicate the location of the faulty antenna elements.

For a linear array with isotropic antenna elements, we consider the array factor instead of the far electric field, which can be written at the $(n+1)^{\text{th}}$ measurement position as follows

$$v_{\text{AF},n+1}^L = \sum_{u=1}^{U} c_u \mathrm{e}^{-jkx_u \sin\theta_n \cos\phi_n} + w_n. \tag{7}$$

Without loss of generality, we assume that the measurements are collected in the $x-z$ plane, i.e., $\phi_n = 0, \ \forall \ n = 0, \ \cdots, \ N-1$. Hence, the ***measurement matrix*** $\mathbf{A}$ is

$$\mathbf{A} = \begin{bmatrix} \mathrm{e}^{-jkx_1 \sin\theta_0} & \mathrm{e}^{-jkx_2 \sin\theta_0} & \cdots & \mathrm{e}^{-jkx_U \sin\theta_0} \\ \vdots & \vdots & \vdots & \vdots \\ \mathrm{e}^{-jkx_1 \sin\theta_{N-1}} & \mathrm{e}^{-jkx_2 \sin\theta_{N-1}} & \cdots & \mathrm{e}^{-jkx_U \sin\theta_{N-1}} \end{bmatrix}.$$

Moreover, the l_2 norm of any column of the measurement matrix is equal to $\sqrt{N}$: $\|\mathbf{A}(:,i)\| = \sqrt{N}, \ \forall \ i \in \{1, \ ..., \ U\}$. After some straightforward manipulations, the inner product between the u^{th} and q^{th} columns of $\mathbf{A}$ can be written as follows

$$|\langle \mathbf{A}(:,u), \mathbf{A}(:,q) \rangle| = \left| \sum_{n=0}^{N-1} \mathrm{e}^{-jk\triangle_{uq} \sin\theta_n \cos\phi_n} \right|. \tag{8}$$

Computing a closed-form expression for the worst-case coherence for a general measurement matrix, $\mathbf{A}$, appears to be too complicated. Therefore, we focus on a uniform linear array (ULA) with inter-element spacing denoted by d_x, which is of high practical interest. Both d_x and $\theta_n, \ n \in \{0, \ \cdots, \ N-1\}$ can be chosen in this case such that $\mathbf{A}$ is constructed from N rows of the discrete Fourier transform (DFT) matrix of size

$U \times U$. For example, for $d_x = \lambda$ and $\sin\theta_n = \frac{n}{U}$, $n \in \{0, \cdots, N-1\}$, the measurement matrix reduces to the first N rows of the DFT matrix of size $U \times U$ and each row corresponds to a particular measurement as follows

$$\mathbf{A} = \begin{bmatrix} 1 & 1 & \cdots & 1 \\ 1 & \mathrm{e}^{-j2\pi\frac{1}{U}} & \cdots & \mathrm{e}^{-j2\pi\frac{U-1}{U}} \\ \vdots & \vdots & \vdots & \vdots \\ 1 & \mathrm{e}^{-j2\pi\frac{(N-1)}{U}} & \cdots & \mathrm{e}^{-j2\pi\frac{(N-1)(U-1)}{U}} \end{bmatrix}. \quad (9)$$

This raises the following interesting question: what is the best set of indices out of $\binom{U}{N}$ in the $U \times U$ DFT matrix to achieve the smallest worst-case coherence? Conducting exhaustive search over all the possible subsets is not feasible, especially for a large number of antenna array elements with a relatively small number of observations. In the next section, we describe two procedures to construct the measurement matrix with low worst-case coherence by judiciously choosing N rows from the $U \times U$ DFT matrix based on [8] and [9].

III. Measurements Procedures

A. Few-Distinct-Inner-Products Measurements Procedure

In this section, we present an algorithm based on the approach outlined in [8]. Our goal is to select N rows out of the full $U \times U$ DFT matrix to minimize the worst-case coherence, where each row represents a particular measurement angle θ_n. The presented algorithm determines the N rows such that the number of *distinct* pairwise inner products is reduced from $\binom{U}{2}$ to $\frac{U-1}{N}$ and it ensures that each such inner product value has the same multiplicity factor. The authors of [8] showed that such measurement matrix has low worst-case coherence and, in certain cases, the Welch bound is achieved.

For a prime number of antenna elements U and assuming that N is any divisor of $U-1$ such that $r = \frac{U-1}{N}$ is an integer, the cyclic group $\mathcal{G} = (\mathbb{Z}/U\mathbb{Z})^{\times}$, the multiplicative group of the integers modulo U, has a unique subgroup, denoted by $\mathcal{K}$, of order m consisting of distinct r^{th} powers of the elements of $\mathcal{G}$. In other words, $\mathcal{K} = \{1,\ k, \cdots,\ k^{N-1}\}$ where $k = g^r$ and g is the unique generator of $\mathcal{G}$. The measurement matrix constructed from rows of the $U \times U$ DFT matrix and indexed by the set $\mathcal{K}$ has at most r distinct inner product values [8]. For example, for $U = 67$ antenna elements and choosing $N = 11$ measurements, i.e., $r = \frac{66}{11} = 3$, the constructed measurement matrix consists of the rows indexed by $\{1,\ 9,\ 14,\ 15,\ 22,\ 24,\ 25,\ 40,\ 59,\ 62,\ 64\}$ and has at most 3 distinct inner product values with an equal multiplicity of $\frac{67^2-67}{3} = 1474$. The algorithm steps are summarized below:

Algorithm 1 Few-Distinct-Inner-Products Measurements Procedure

1: Find the unique generator g for $(\mathbb{Z}/U\mathbb{Z})^{\times}$.
2: Choose the number of measurements N to be any divisor of $U-1$.
3: The set of rows' indices is given by $\{1,\ k,\ \cdots,\ k^{m-1}\} \mod U$, where $k = g^{\frac{U-1}{N}}$.

It is worth mentioning that the measurement matrix in this case achieves the Welch bound if and only if the set $\mathcal{K}$ forms a difference set in $(\mathbb{Z}/U\mathbb{Z})^{\times}$ [11]. For instance, if $r = 2$ and $N-1$ is not dividable by 4, then the Welch bound is achieved [8].

In this algorithm, the number of measurements, N, is restricted to be one of the factors of $U-1$. In some cases, N approaches half the number of antenna elements which is considered too many measurements. For example, assuming $U = 107$, then $N \in \{1,\ 2,\ 53,\ 106\}$ which is either too few measurements to reliably recover the defective antenna elements or too many measurements.

B. Polynomial-Based Measurements Procedure

Next, to overcome the drawback of Algorithm 1, we present an alternative algorithm that can be used for any number of measurements. In scenarios where both algorithms can construct the measurement matrix, the one obtained by Algorithm 1 exhibits smaller worst-case coherence, as will be numerically verified in Section IV.

The procedure for this algorithm is similar to the algorithm described in [9]. For prime U, construct the multiset $\mathcal{T} = \{Q(m) \mod U :\ m = 1,\ 2,\ \cdots,\ M\}$ where M is an integer greater than 1 and $Q(m)$ is an R-degree polynomial with $R \geq 2$ and coefficients denoted by $\{\alpha_i\}_{i=1}^{R}$: $Q(m) = \alpha_1 m + \cdots + \alpha_R m^R$. Those coefficients are chosen to be co-prime to U, i.e., $\alpha_R \in \{1,\ \cdots,\ U-1\}$ while the other coefficients $\{\alpha_i\}_{i=1}^{R-1} \in \{0,\ 1,\ \cdots,\ U-1\}$. The set of row indices corresponds to the unique elements in $\mathcal{T}$. It is worth mentioning that M is chosen big enough such that the multiset $\mathcal{T}$ has N unique elements. The entire procedure for selecting the measurements is outlined below:

Algorithm 2 Polynomial-Based Measurements Procedure

1: Select integer $R \geq 2$.
2: Select $\alpha_R \in \{1,\ 2,\ \cdots,\ U-1\}$ relatively prime to U and $\{\alpha_i\}_{i=1}^{R-1} \in \{0,\ 2,\ \cdots,\ U-1\}$.
3: Construct $Q(m) = \alpha_1 m + \cdots + \alpha_R m^R$.
4: Choose integer $M \geq 1$ and form the multiset of integers $\mathcal{T} = \{Q(m) \mod U :\ m = 1,\ 2,\ \cdots,\ M\}$.
5: Select the N rows' indices to be unique elements of $\mathcal{T}$.

IV. Numerical Results

To evaluate the performance, we define detection probability as follows: $P_{\text{D}} = \frac{|\hat{\mathcal{S}} \cap \mathcal{S}|}{\kappa}$, where κ is the number of defective antenna elements that the CS recovery algorithm tries to recover, while $\mathcal{S}$ and $\hat{\mathcal{S}}$ are the sets of true and estimated indices of the defective antenna elements, respectively. The quantity $|\hat{\mathcal{S}} \cap \mathcal{S}|$ determines the number of correctly identified faulty antenna elements. Moreover, we define SNR $= \frac{\mathbf{c}_{\text{T}}^H \mathbf{c}_{\text{T}}}{\sigma_w^2}$.

To recover $\tilde{\mathbf{c}}$ from (6), several approaches have been proposed in the CS literature to convert the problem in (2) into a convex optimization problem by replacing the l_0 norm by the l_1 norm or other greedy algorithms with low complexity. Here, we focus on a well-known greedy algorithm, namely the orthogonal matching pursuit (OMP), that iteratively finds the most correlated column of the measurement matrix $\mathbf{A}$ and the corresponding entry in $\mathbf{c}$ until κ entries are recovered.

Unless stated otherwise, we consider a ULA with inter-element spacing of λ and the angular space is sampled such that $\sin\theta_n \in \{0, \cdots, \frac{U-1}{U}\}$, $\forall\ n \in \{0, \cdots, N-1\}$. The algorithms in Section III enable one to select the N measurements to reduce the worst-case coherence and improve the reliability of recovering the faulty antenna elements. Moreover, the number of faulty elements is set to be 4% of the total number of antenna elements and their excitation coefficients are set equal to zero. For simplicity, the excitation coefficients of the fault-free antenna elements are set to 1.

Figure 1 shows the detection probability for a ULA with $U = 941$ antenna elements where 38 are defective antenna elements and 235 measurements are collected. In this figure, we compare between Algorithm 1 with the generator $g = 2$ and uniform sampling of the elevation angle, i.e., θ_n being equal to $\frac{2\pi n}{N}$ with $n \in \{0, \ldots, N-1\}$. The constructed matrix using Algorithm 1 achieves a lower worst-case coherence of $\mu = 0.0717$ than the one constructed using uniform sampling, for which $\mu = 0.22$. At high SNR, the detection probability using Algorithm 1 increases from 75% to 97%. To further assess the performance of Algorithm 1, we also compare it with a random measurements collection procedure where the measurements correspond to a partial DFT matrix with the rows selected uniformely at random, which is known to satisfy near-optimal RIP guarantees [9]. It is evident from this figure that the detection probability using Algorithm 1 is close to the performance achieved by random measurements collection.

Next, Figure 2 shows the detection probability versus the number of defective antenna elements κ. At detection probability of 90%, Algorithm 1 identifies 58 faulty antenna elements compared with only 14 faulty elements when uniformly-sampled measurements are used, while it approaches the performance of random measurements collection.

When the number of measurements, N, is not a divisor of $U-1$, Algorithm 2 can used to construct the measurement matrix with low μ. We consider the same antenna array size of $U = 941$ and $N = 230$, for which $\frac{U-1}{N}$ is not integer. For the R-degree polynomial, we choose $R = 2$ and set $\{\alpha_i\}_{i=1}^{R} = 1$ as in [9]. The constructed measurement matrix exhibits lower worst-case coherence of $\mu = 0.113$, compared to uniform elevation angle sampling with $\mu = 0.3073$ and it achieves higher detection probability. Also, it gets closer to the near-optimal performance of random measurements collection as shown in Figure 3.

Table I shows the worst-case coherence for measurement matrices constructed by Algorithms 1 and 2. It shows that Algorithm 1 achieves lower worst-case coherence or even the Welch bound in some cases. However, it can only be applied when $\frac{U-1}{N}$ is an integer. On the other hand, Algorithm 2 has more parameters to control such as the polynomial order R and its coefficients $\{\alpha_i\}_{i=1}^{R}$, which gives it greater flexibility for any number of measurements N.

In Figure 4, we quantify the detection probability for different $\delta = \frac{N}{U}$ and $\rho = \frac{\kappa}{N}$, where δ and ρ are the normalized indeterminacy and sparsity levels. This figure can be called the detection probability phase transition figure (PTF) [12] because it shows the transition from the upper-left corner representing recovery failure to the lower-right corner for successful recovery in a noise-free scenario. As shown in Figure 4a, uniform sampling results in poor performance at high sparsity levels. On the other hand, Figure 4b shows similar detection probability region for Algorithm 2 as the random measurements collection procedure in Figure 4c. It is worth mentioning that the detection probability PTF for Algorithm 1 is less informative because only few points can be generated since the number of measurements has to be a divisor of the number of antennas -1, which restricts ρ and δ to specific values.

TABLE I: The worst-case coherence for different ULA sizes.

$(U,\ N)$	Algorithm 1	Algorithm 2	Welch bound
(67, 11)	0.344	0.473	0.278
(73, 9)	**0.314**	0.540	**0.314**
(941, 235)	0.072	0.102	0.057

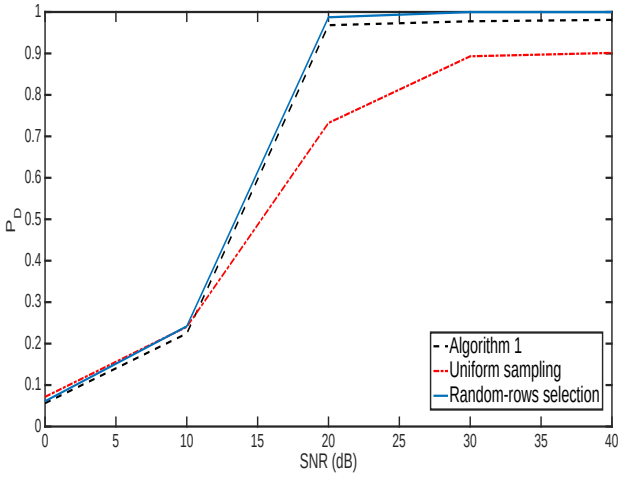

Fig. 1: Detection probability versus SNR (dB) for ULA of 941 antenna elements and 235 measurements, corresponding to different measurement collection procedures.

V. Conclusion

In this paper, we presented two algorithms to construct the measurement matrix for a massive MIMO ULA to enhance the reliability of antenna array diagnosis based on CS principles and increase the detection probability of the faulty antenna elements. We showed that uniformly taking the measurements results in inferior performance compared with carefully-designed deterministic measurements. In most scenarios, the presented algorithms either achieved the Welch lower-bound or came very close to it. Finally, we presented extensive numerical simulations to quantify the performance gains of the presented algorithms.

There is significant room to improve the performance of our proposed techniques. For instance, the excitation coefficients vector, $\mathbf{c}$, can be optimized to enhance the detection probability. For Algorithm 2, the polynomial order and its coefficients can be further investigated and optimized.

In our future work, we will also generalize this work to nonuniform linear arrays, study two-dimensional (2D) antenna array elements and extend the presented algorithms to select the best N rows out of a $U \times U$ 2D DFT matrix.

Acknowledgement: The authors thank Dr. Raed Shubair form Khalifa University for useful discussions throughout the course of this work.

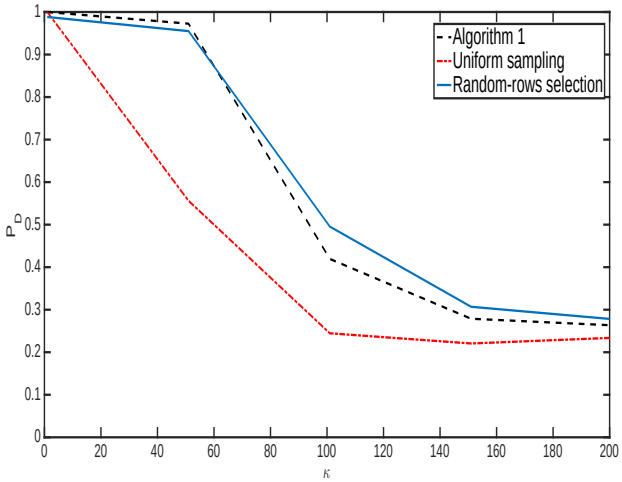

Fig. 2: Detection probability versus the number of defective antenna elements at SNR=40dB for ULA of 941 antenna elements and 235 measurements.

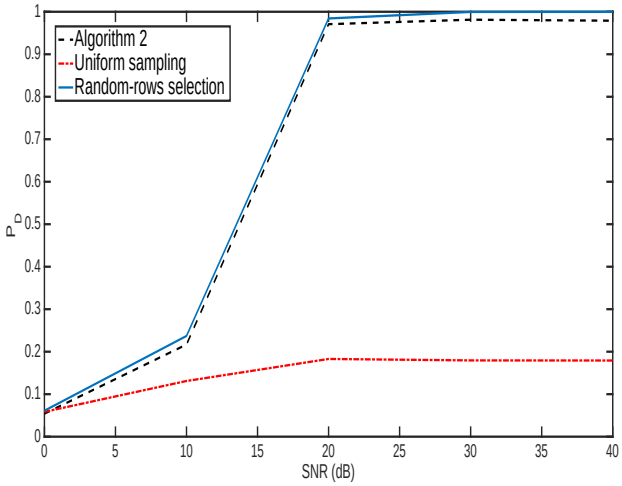

Fig. 3: Detection probability versus SNR (dB) for ULA of 941 antenna elements and 230 measurements.

REFERENCES

[1] Y. H. Nam, B. L. Ng, K. Sayana, Y. Li, J. Zhang, Y. Kim, and J. Lee, "Full-Dimension MIMO (FD-MIMO) for Next Generation Cellular Technology," *IEEE Comm. Mag.*, vol. 51, no. 6, pp. 172–179, June 2013.

[2] J. J. Lee, E. M. Ferren, D. P. Woollen, and K. M. Lee, "Near-Field Probe Used as a Diagnostic Tool to Locate Defective Elements in an Array Antenna," *IEEE Transactions on Antennas and Propagation*, vol. 36, no. 6, pp. 884–889, Jun 1988.

[3] O. M. Bucci, M. D. Migliore, G. Panariello, and P. Sgambato, "Accurate Diagnosis of Conformal Arrays from Near-Field Data Using the Matrix Method," *IEEE Transactions on Antennas and Propagation*, vol. 53, no. 3, pp. 1114–1120, March 2005.

[4] A. Buonanno and M. D'Urso, "A Novel Strategy for the Diagnosis of Arbitrary Geometries Large Arrays," *IEEE Transactions on Antennas and Propagation*, vol. 60, no. 2, pp. 880–885, Feb 2012.

[5] M. D. Migliore, "A Compressed Sensing Approach for Array Diagnosis From a Small Set of Near-Field Measurements," *IEEE Transactions on Antennas and Propagation*, vol. 59, no. 6, pp. 2127–2133, June 2011.

[6] G. Oliveri, P. Rocca, and A. Massa, "Reliable Diagnosis of Large Linear Arrays; A Bayesian Compressive Sensing Approach," *IEEE Trans. on Anten. and Propag.*, vol. 60, no. 10, pp. 4627–4636, Oct 2012.

[7] M. Carlin, G. Oliveri, and A. Massa, "Planar Array Diagnosis Through Compressive Sensing: A Preliminary Assessment," in *The 8th European Conference on Antennas and Propagation*, April 2014, pp. 399–402.

[8] M. Thill and B. Hassibi, "Group Frames With Few Distinct Inner Products and Low Coherence," *IEEE Transactions on Signal Processing*, vol. 63, no. 19, pp. 5222–5237, Oct 2015.

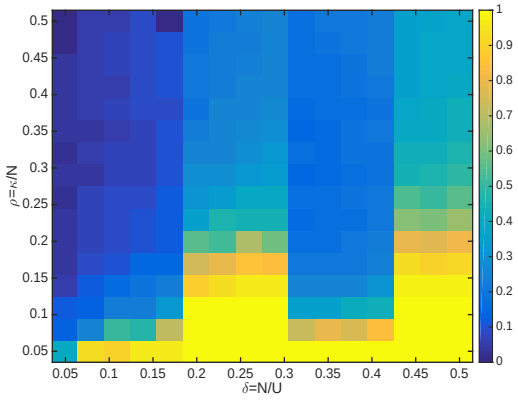

(a) Uniform sampling algorithm

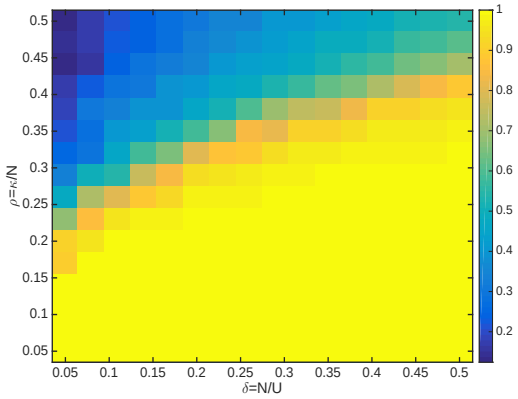

(b) Algorithm 2

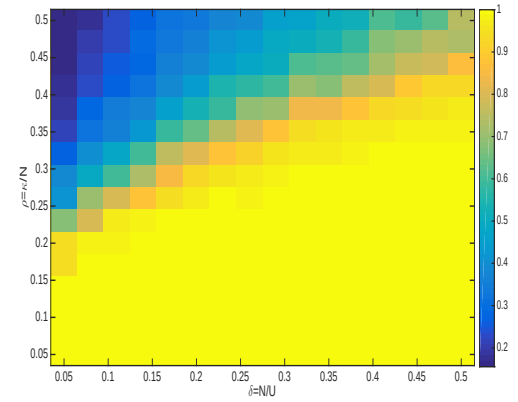

(c) Random-rows selection

Fig. 4: Detection probability phase transtions for $U = 941$.

[9] L. Applebaum, W. U. Bajwa, A. R. Calderbank, J. Haupt, and R. Nowak, "Deterministic Pilot Sequences for Sparse Channel Estimation in OFDM Systems," in *IEEE 17th International Conference on Digital Signal Processing (DSP)*, July 2011, pp. 1–7.

[10] W. U. Bajwa, R. Calderbank, and S. Jafarpour, "Why Gabor frames? Two Fundamental Measures of Coherence and Their Role in Model Selection," *Journal of Communications and Networks,*, vol. 12, no. 4, pp. 289–307, Aug 2010.

[11] P. Xia, S. Zhou, and G. B. Giannakis, "Achieving the Welch Bound with Difference Sets," *IEEE Transactions on Information Theory*, vol. 51, no. 5, pp. 1900–1907, May 2005.

[12] A. Maleki and D. L. Donoho, "Optimally Tuned Iterative Reconstruction Algorithms for Compressed Sensing," *IEEE Journal of Selected Topics in Signal Processing*, vol. 4, no. 2, pp. 330–341, April 2010.